

## Tonoplast Anion Channel Activity Modulation by pH in *Chara corallina*

G. Berecki<sup>1,2</sup>, M. Eijken<sup>2</sup>, F. Van Iren<sup>2</sup>, B. Van Duijn<sup>1</sup>

<sup>1</sup>Center for Phytotechnology LU/TNO, TNO Department of Applied Plant Sciences, Wassenaarseweg 64, 2333AL Leiden, The Netherlands

<sup>2</sup>Center for Phytotechnology LU/TNO, Institute of Molecular Plant Sciences, Leiden University, Leiden, The Netherlands

Received: 14 March 2001/Revised: 16 July 2001

**Abstract.** The patch-clamp technique was used to investigate regulation of anion channel activity in the tonoplast of *Chara corallina* in response to changing proton and calcium concentrations on both sides of the membrane. These channels are known to be  $\text{Ca}^{2+}$ -dependent, with conductances in the range of 37 to 48 pS at pH 7.4. By using low pH at the vacuolar side (either  $\text{pH}_{\text{vac}}$  5.3 or 6.0) and a cytosolic pH ( $\text{pH}_{\text{cyt}}$ ) varying in a range of 4.3 to 9.0, anion channel activity and single-channel conductance could be reversibly modulated. In addition,  $\text{Ca}^{2+}$ -sensitivity of the channels was markedly influenced by pH changes. At  $\text{pH}_{\text{cyt}}$  values of 7.2 and 7.4 the half-maximal concentration ( $EC_{50}$ ) for calcium activation was 100–200  $\mu\text{M}$ , whereas an  $EC_{50}$  of about 5  $\mu\text{M}$  was found at a  $\text{pH}_{\text{cyt}}$  of 6.0. This suggests an improved binding of  $\text{Ca}^{2+}$  ions to the channel protein at more acidic cytoplasm. At low  $\text{pH}_{\text{cyt}}$ , anion channel activity and mean open times were voltage-dependent. At pipette potentials ( $V_p$ ) of +100 mV, channel activity was approximately 15-fold higher than activity at negative pipette potentials and the mean open time of the channel increased. In contrast, at  $\text{pH}_{\text{cyt}}$  7.2, anion channel activity and the opening behavior seemed to be independent of the applied  $V_p$ . The kinetics of the channel could be further controlled by the  $\text{Ca}^{2+}$  concentration at the cytosolic membrane side: the mean open time significantly increased in the presence of a high cytosolic  $\text{Ca}^{2+}$  concentration. These results show that tonoplast anion channels are maintained in a highly active state in a narrow pH range, below the resting  $\text{pH}_{\text{cyt}}$ . A putative physiological role of the pH-dependent modulation of these anion channels is discussed.

**Key words:** *Chara* — Tonoplast —  $\text{Ca}^{2+}$ -activated an-

ion channel — pH — Voltage dependence — Open-time constant

### Introduction

Calcium is a ubiquitous second messenger in all plant cells (Gilroy, Bethke & Jones, 1993; McAinsh, 1990; Schroeder & Hagiwara, 1989), but its action depends on a complex network of signaling molecules, including protons. Although recognized earlier (Blatt, 1987; Kurkdjian & Guern, 1989; Felle, 1989), the messenger role of protons was less studied in plant cell signal transduction cascades, and the upstream events of  $\text{H}^+$  signaling are not yet revealed (Grabov & Blatt, 1998). Cytosolic calcium ( $[\text{Ca}^{2+}]_{\text{cyt}}$ ) and  $\text{H}^+$  concentrations ( $\text{pH}_{\text{cyt}}$ ) are known to be modulated by many endogenous compounds, physiological and stress stimuli (Kinnersley & Turano, 2000). In signaling pathways crosstalk, cytosolic  $[\text{Ca}^{2+}]$  is coupled to the  $\text{pH}_{\text{cyt}}$ . For instance, a decrease of  $\text{pH}_{\text{cyt}}$  can result in a rise of the  $[\text{Ca}^{2+}]_{\text{cyt}}$  (Felle, 1988; Grabov & Blatt, 1997; Plieth, Sattelmacher & Hansen, 1997), indicating that changes in  $[\text{Ca}^{2+}]_{\text{cyt}}$  and  $\text{pH}_{\text{cyt}}$  may act in the same signal transduction chains.

Ion channels are potential targets to be regulated by calcium and protons. While pH-dependence of plasma membrane cation channels was studied in many different cell types (for an overview see Grabov & Blatt, 1998; Keunecke & Hansen, 2000), modulation of vacuolar cation channels by pH in plants has only been described for the  $\text{Ca}^{2+}$ - and  $\text{K}^+$ -permeable slow vacuolar (SV) channel (Allen & Sanders, 1996; Schultz-Lessdorf & Hedrich, 1995; Ward & Schroeder, 1994) and vacuolar  $\text{K}^+$ -selective (VK) channels of guard cells (Allen, Amtmann & Sanders, 1998). Much less is known about pH-regulation of plant anion channels, which play important roles in the control of membrane excitability, modulation of osmotic stress response and signal transduction, regu-

lation of cell volume and intracellular pH. The *Vicia faba* guard cell anion channel (GCAC1) recognizes pH gradients across the plasma membrane, being activated by cytoplasmic ATP in a pH-dependent manner (Schultz-Lessdorf, Lohse & Hedrich, 1996).

We are interested in the role and regulation of vacuolar channels in the algae *Chara corallina*. In *Chara* cells proton- and  $\text{Ca}^{2+}$ -buffer mechanisms provide short- and long-term regulation of the homeostasis of these messengers (Plieth et al., 1997). The cytoplasmic and vacuolar pH values are shown to be in the range of 7.4–7.8 and 5.0–6.6, respectively. Low vacuolar pH, necessary for vacuolar functions, is maintained by two acidifying membrane proteins, the vacuolar ATPase (V-ATPase) and the vacuolar pyrophosphatase (V-PPase). Altered  $\text{H}^+$  concentrations modulate not only the activity of these pumps (Moriyasu, Shimmen & Tazawa, 1984; Takeshige, Tazawa & Hager, 1988) but the gating of the tonoplast  $\text{K}^+$  channels as well. These maxi-K channels are activated by low  $[\text{Ca}^{2+}]_{\text{cyt}}$  and blocked by a  $[\text{Ca}^{2+}]_{\text{cyt}}$  above 100  $\mu\text{M}$  (Laver & Walker, 1991). They show the highest activity at a pH of 8.5, while at low pH values their activity reversibly decreases in a cooperative protonation process. Both low  $\text{pH}_{\text{cyt}}$  and  $\text{pH}_{\text{vac}}$  reduce channel open probabilities towards zero, without affecting single channel conductance. A Hill equation, fitted to the  $\text{pH}_{\text{cyt}}$ -dependent inhibition kinetics, resulted in a Hill coefficient of  $n = 2.05$  and an apparent dissociation constant,  $\text{p}K_a$  of 6.6 (Lühring, 1999). In addition, low  $\text{pH}_{\text{vac}}$  strongly shifted the voltage sensitivity towards depolarized voltages. Therefore,  $\text{H}^+$  can be regarded as a significant modulator of the channel, although the distinction between a channel modulator and a principal ligand seems to be merely speculative.

Reported relatively early (Tyerman & Findlay 1989), the anion channels of the *Chara* tonoplast are only studied in more detail recently. Cytoplasmic  $\text{Ca}^{2+}$  has been shown to modulate anion channel activity from the cytosolic but not from the vacuolar side of the membrane. Increasing calcium concentrations raise activity of these channels (Berecki et al., 1999). In principle, the presence of such a conductance has been anticipated in higher plants and must occur in acidic vesicles to maintain electroneutrality (Glickman et al., 1983). Regarding  $\text{Ca}^{2+}$ -sensitivity, there is some overlap in characteristics of the *Chara* tonoplast anion channel with vacuolar channels of higher plants, although most higher plant vacuolar channels are quite impermeable to anions. On the other hand, *Chara* tonoplast anion channels have distinctive properties, featuring two types of channel activities. In droplet-attached configuration of the patch-clamp technique, the channel often rectifies outward current flow, while rectification ceases when the membrane patch is excised and held at a pipette potential ( $V_p$ ) of 0 mV in symmetrical solutions, suggesting that the nonlin-

ear current-voltage relationship of the channel depends on the long-term tonoplast transmembrane potential (i.e., on the preconditioning  $V_p$ ) (Berecki et al., 1999). The aim of the present study was to investigate the influence of pH on the  $\text{Ca}^{2+}$ -activated anion channel. In addition, the effects of pH changes on  $\text{Ca}^{2+}$  sensitivity and voltage dependence were tested. Experiments were performed on excised inside-out patches originating from cytoplasmic droplets, with control of the chemical composition of solutions at both the cytosolic and vacuolar sides of the membrane.

## Materials and Methods

### PLANT MATERIAL AND ISOLATION OF CYTOPLASMIC DROPLETS

Internodal cells of *Chara corallina* were cultured as described before (Berecki et al. 1999). For droplet isolation, intracellular perfusion of the cell was carried out, using a modification (Berecki et al., 1999) of the method of Tazawa & Kikuyama & Shimmen (1976). Recently we have shown that the orientation of the droplet membrane depends on the applied isolation procedure (Berecki et al., 2001). The procedure used here reproducibly yielded cytoplasmic droplets with the cytosolic side of the membrane facing the inside part of the droplet. Shortly, the cell was blotted dry with a tissue paper and laid on a Parafilm covered glass slide. Water evaporation resulted in loss of turgor within 3 to 5 minutes. 30–40  $\mu\text{L}$  bath solution was pipetted on both ends of the cell and each cell end was removed with a pair of scissors. The glass was tilted back and forth in such a way that the bath medium flowed through the cell, sweeping out the content of the cell, resulting in a suspension of cytoplasmic droplets. Droplets with diameters in the range of 20  $\mu\text{m}$  to 200  $\mu\text{m}$  were formed and collected in an Eppendorf vial for storage. Typically 10–20  $\mu\text{L}$  of this suspension was transferred into the experimental chamber, which was placed on the stage of an inverted phase-contrast microscope (Nikon Diaphot-TMD, Japan). Subsequently, 480  $\mu\text{L}$  bath solution was added carefully to avoid turbulence. The bath solution was exchanged 3 to 4 times to ensure that the strong buffer capacity of the cell contents did not change the fixed pH. The pH of the resulting suspensions was routinely checked after experiments, by collecting the content of the bath chamber in an Eppendorf tube, followed by measuring the pH with a pH electrode (Sensorex, Stanton, CA.).

### SOLUTIONS

Salt solutions were prepared from 0.1 or 1 M stock solutions with MilliQ water and filtered (Millipore S.A., Molsheim, France, type 0.22  $\mu\text{m}$ ) before use. The chemicals used were purchased from Merck (Darmstadt, Germany) and Sigma (St. Louis, MO.). The compositions of the experimental solutions are shown in Tables 1 and 2. By using  $\text{Cs}^+$  in the bath and pipette solutions the  $\text{K}^+$ -channels were blocked (Klieber & Gradmann, 1993; Berecki et al., 1999) and only anion channel currents were recorded.

### SINGLE-CHANNEL RECORDING

Patch pipettes with internal filaments (Clark Electromedical Instruments, Pangbourne Reading, England, type GC150TF-15) were pulled with a Narishige two-stage puller (Tokyo, Japan, Model PB-7) and

**Table 1.** Composition of solutions used to determine  $\text{Ca}^{2+}$ - and voltage-dependence

pH	CsCl mM	HEPES/ Tris mM	MES <sup>b</sup> mM	EGTA mM	$\text{CaCl}_2$ $\mu\text{M}$	Free $\text{Ca}^{2+}$ <sup>c</sup> $\mu\text{M}$
5.3 <sup>a</sup>	140		10		100	
6.0 <sup>a</sup>	140		10		100	
6.0	135		10	10	14	0.05
6.0	137.5		10	5	70	0.5
6.0	137.5		10	5	170	1.3
6.0	137.5		10	5	260	2
6.0	140		10		5, 10, 13, 50, 100, 500	
7.2	138	10		2	800	0.1
7.2	140	10			1, 10, 30, 50, 100, 300, 500, 1000	
7.4	140	10			30, 50	

<sup>a</sup> Pipette solutions<sup>b</sup> MES-buffers were adjusted with NaOH to the indicated pH-values.<sup>c</sup> Free  $\text{Ca}^{2+}$ -concentrations in the presence of a single chelating ligand were computed using the program Ligandy (developed by P. Tatham and B. Gomperts, University College, London).**Table 2.** Composition of solutions used to determine pH- and voltage-dependence

Solution	pH	CsCl mM	MES/Tris mM	$\text{CaCl}_2$ $\mu\text{M}$
Pipette	5.3, 6.0	140	10	100
Bath	4.1, 4.3, 5.0, 5.3, 5.5, 6.0, 6.3, 6.6, 6.9, 7.2, 7.4, 7.7, 8.0, 8.6 or 8.9	140	10	50

fire-polished, resulting in a tip resistance of 6–10 M $\Omega$  when filled with experimental solutions. Currents were recorded at room temperature ( $23 \pm 2^\circ\text{C}$ ) with an Axopatch 200 Amplifier (Axon Instruments, Foster City, CA), using conventional voltage-clamp techniques according to Hamill et al. (1981). Data acquisition and control of the amplifier were performed with pCLAMP 7.0 in combination with a Digidata 1200A interface, while data analysis was performed with the pCLAMP 6.0 software package (Axon Instruments). Signals were digitized at 5 kHz and filtered at 1 kHz with a 4-pole lowpass Bessel filter. The pipette potential ( $V_p$ ) was measured with respect to the bath potential (ground). Junction potentials were balanced before the formation of each giga-seal.

Excising a patch from the cytoplasmic droplet-attached configuration resulted in the inside-out patch configuration (cytosolic side of the membrane facing the bath solution). Thus, the cytosolic side of the tonoplast could be controlled by the composition of the bath solution. Perfusion of the bath was only applied during experiments shown in Fig. 1, through the single outlet barrel of a homemade double-inlet perfusion port, that was attached to 2 different reservoirs among which selections could be made. By micromanipulation, the perfusion barrel was placed approximately 100  $\mu\text{m}$  from the patch under study. In these experiments, the original (500  $\mu\text{l}$ ) experimental chamber was replaced with a smaller, 100  $\mu\text{l}$  volume chamber, resulting in a faster exchange of the bath solution, while perfusion and waste withdrawal were done

at equal rate ( $\pm 10 \mu\text{l}/\text{sec}$ ). In all other cases perfusion was omitted and the  $\text{Ca}^{2+}$ - and pH-dependence of the anion current were tested in the presence of fixed  $\text{Ca}^{2+}$  and  $\text{H}^+$  concentrations.

According to convention (Bertl et al. 1992), outward anion currents are cytosolic-side directed and are graphically represented as downward, while inward anion currents are represented as upward deflections.

## DATA ANALYSIS

### Single-channel Conductance

Single-channel amplitude values were obtained both by fitting all-points histograms with Gaussian functions and measuring the distance between the midpoints of the histogram bins or by measuring the distance between two lines, one set on the baseline noise, considered 0 pA, and the other set on the noise of the open level. In both cases the resulting single-channel current amplitude values were used to calculate single-channel conductance ( $G$ ), with the use of  $E$  (applied electromotive force) =  $V_p$  (pipette potential) –  $E_{\text{rev}}$  (calculated reversal potential).

### Channel Activity

In most cases, more than one channel was active within a patch; the observed single-channel open levels varied from 1 to 9 (*data not shown*). The term channel activity ( $NP_o$ ) was introduced to estimate open probability ( $P_o$ ) of all ( $N$ ) single channels within a patch:

$$NP_o = \sum_{n=1}^N np_n = 1p_1 + 2p_2 + 3p_3 + \dots + Np_N \quad (1)$$

where,  $NP_o$  was calculated using amplitude analysis of the baseline level and of the various open levels of the channel to create an amplitude histogram. The histogram was then fitted with a sum of Gaussian distributions to calculate  $p_n$  (according to Hille, 1992), the probability that  $n$  channels are open simultaneously. Activity in each case was calculated from at least 30 sec of recording starting 2–3 min after establishing the inside-out patch configuration.

### Dose-dependence

Averaged data points from at least 3 independent experiments were fitted in Origin (Microcal Software, Northampton, MA.), with Hill equations of the type:

$$(NP_o)_{\text{rel}} = \frac{[H^+]^{n_1} \cdot [H^+]^{(-n_2)}}{\{K_{a_1}^{n_1} + [H^+]^{n_1}\} \cdot \{K_{a_2}^{(-n_2)} + [H^+]^{(-n_2)}\}} \quad (2)$$

where  $K_{a_1}$  and  $K_{a_2}$  represent the apparent dissociation constants of the activation and deactivation binding sites of  $\text{H}^+$ , while  $n_1$  and  $n_2$  are the corresponding Hill coefficients indicating the number of binding sites and, in case of  $n > 1$ , a cooperative type of  $\text{H}^+$  binding, respectively.

$$NP_o = (NP_o)_{\text{max}} \cdot \frac{[\text{Ca}^{2+}]^n}{K_a^n + [\text{Ca}^{2+}]^n} \quad (3)$$

where,  $K_a$  represents the apparent dissociation constant of the activation binding sites of  $\text{Ca}^{2+}$ ,  $n$  the Hill coefficient and  $(NP_o)_{\text{max}}$  the maximal channel activity.

However, for the data reported here, Eqs. 2 and 3 should be regarded as useful empirical curve-fitting relationships rather than as

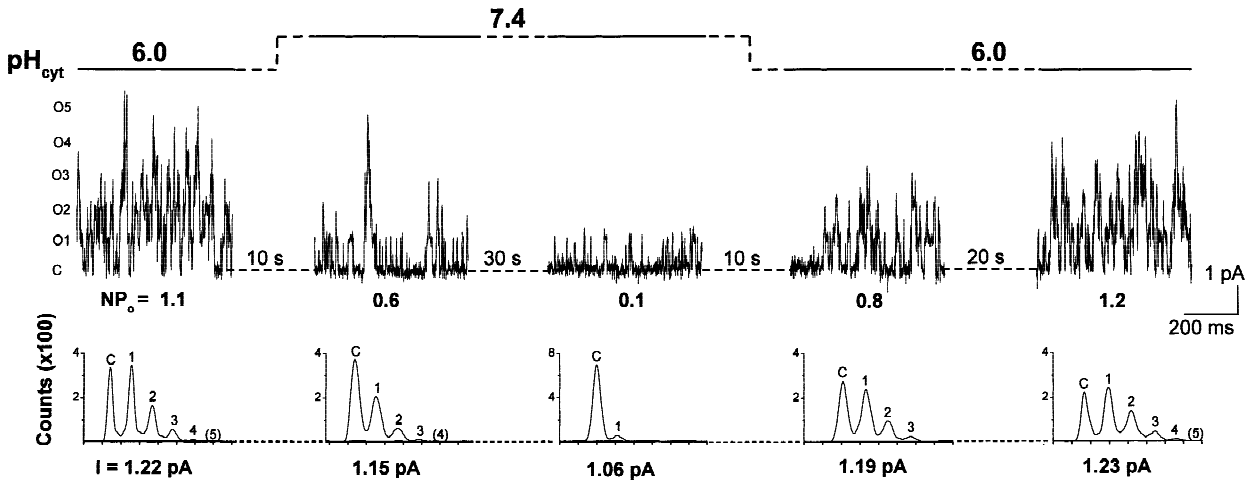


**Fig. 1.** Cytosolic pH ( $\text{pH}_{\text{cyt}}$ ) modulates the activity of single tonoplast anion channels. Representative recordings from excised inside-out patch configuration at  $V_p = +20$  mV show channel activities at  $\text{pH}_{\text{cyt}}$  6.0 before, 5 and 35 sec after perfusion with a  $\text{pH}_{\text{cyt}}$  7.4 solution, respectively. Subsequently, perfusion with a  $\text{pH}_{\text{cyt}}$  6.0 solution is shown. Channel openings are represented by upward deflections, O1, ... O5 = open levels, C = closed level. The composition of the pipette solution of pH 6.0 and that of the bath, buffered at either pH 7.4 or 6.0 (wash), is identical to the composition of solutions shown in Table 2,  $\text{pH}_{\text{vac}} = 6.0$ . An increase in the  $\text{pH}_{\text{cyt}}$  from pH 6.0 to pH 7.4 resulted in a reversible decrease in the activity ( $\text{NP}_o$ , as indicated below each current trace) ( $N = 6$ ). All-points histograms of this particular experiment were generated from 5-sec long recordings. Superimposed individual channel openings are represented by equidistant peaks and numbered continuously. Numbers are given between parentheses if the peak was too small to be fitted properly. The distances between the peaks ( $I$ , current in pA) representing the closed (C) and the first open level ( $I$ ) is indicated below the x-axes of the histograms.

indicators of a particular model of ligand binding (Koshland, Némethy & Filmer, 1966).

### Open-time Distributions

Open-time distribution studies were performed on patch recordings lasting at least 30 sec and showing preferably one open channel. In our experiments, this was obtained more readily by using  $\text{pH}_{\text{vac}}$  of 5.3 (as indicated by the lower  $\text{NP}_o$  values shown in Fig. 2). However, in many cases, patches showed multiple levels even if the  $P_o$  was low. Data from these patches were also included into analysis, provided that the frequency of overlapping events was low. Transitions between the closed and open states were identified using half-amplitude event detection (Colquhoun & Sigworth, 1983). No attempt to correct open times for missed closures was made. Events list files were formed by visual inspection of the data and manually accepting or rejecting putative events, while ignoring events  $< 0.5$  msec in duration. Then, data in the events list were sorted into histogram bins, and fit with single- or double-exponential functions, using maximum likelihood optimization of a Simplex algorithm (Sigworth & Sine, 1987). Consequently, we used the Schwartz criterion to assess model fit (Schwartz, 1978).

### Statistics

Different measurements were compared using Student's  $t$ -test and differences were considered significant at the  $P < 0.05$  level. All values are reported as means  $\pm$  SEM. ( $N$ , number of inside-out patch configurations tested).

## Results

### pH-DEPENDENT ANION CHANNEL ACTIVITY

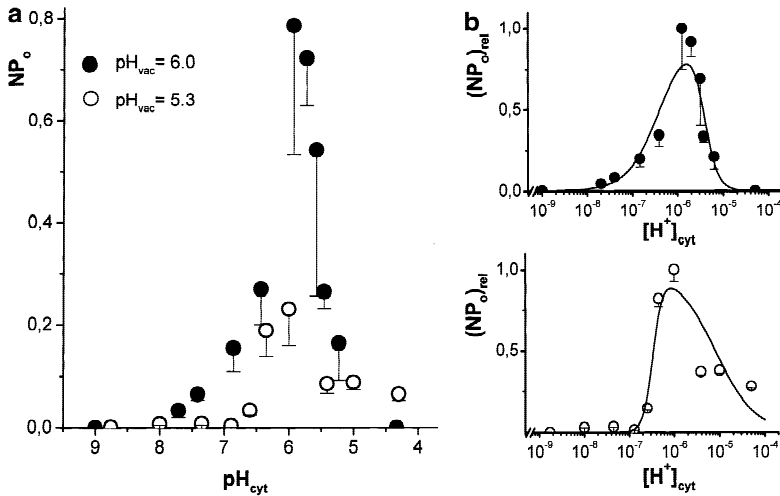
Single tonoplast anion channels of *Chara* showed high steady-state activity in inside-out patches in a  $\text{pH}_{\text{cyt}}$  6.0

bath solution. After recording the basal single-channel activity ( $\text{NP}_o$ ), a solution with  $\text{pH}_{\text{cyt}}$  7.4 was applied to the patch by continuous perfusion. Channel activity gradually decreased to a relatively low level. Then, after returning to the original  $\text{pH}_{\text{cyt}}$  of 6.0, channel activity reverted to control levels within 30 sec. This pH effect was reversible; a second application of the same solutions caused a similar modulation (*data not shown*). Alkalinization reduced both the number of active single channels in the patch and the single-channel current amplitude, as detected by the decreasing number of detected single-channel open levels and by the smaller peak-to-peak distance values, as measured between the midpoints of the histogram bins (Fig. 1).

To further investigate the effects of cytosolic acidification or alkalinization on the anion channel activity, the composition of the pipette solution (vacuolar side) was kept constant at a  $\text{pH}_{\text{vac}}$  of either 5.3 or 6.0, while the  $\text{pH}_{\text{cyt}}$  was varied in a pH range between 4.3 and 9.0, in the presence of  $50 \mu\text{M} [\text{Ca}^{2+}]_{\text{cyt}}$  (see Table 2). Fig. 2a summarizes channel activities ( $\text{NP}_o$ ) as a function of  $\text{pH}_{\text{cyt}}$ . The various  $\text{NP}_o$  values were calculated according to Eq.1. Few channel openings were present at an alkaline  $\text{pH}_{\text{cyt}}$ , while, with decreasing  $\text{pH}_{\text{cyt}}$ ,  $\text{NP}_o$  increased in a dose-dependent manner, showing a maximum at about  $\text{pH}_{\text{cyt}}$  6.0 for both  $\text{pH}_{\text{vac}}$  5.3 and 6.0. Upon further  $\text{pH}_{\text{cyt}}$  reduction below 6.0 the activity decreased and ceased completely at very low  $\text{pH}_{\text{cyt}}$  values.

Assuming the presence of (at least) two cytosolic regulatory sites, channel activation and inhibition as a function of cytosolic acidification could be described by





Eq. 2 (Fig. 2b, solid lines), showing a bell-shaped pH dependence at  $pH_{vac}$  5.3 and  $pH_{vac}$  6.0, respectively. The fit at  $pH_{vac}$  5.3 (open circles) resulted in a  $pK_{a1}$  of 6.47 and  $n_1 = 4$ , indicating a marked positive cooperativity, as channel activity significantly changed over a relatively small range of  $[H^+]_{cyt}$ . Further protonation reduced  $NP_o$ , the low- $pH_{cyt}$ -dependent inhibition kinetics of the channel resulting in a  $pK_{a2}$  of 5.07 and  $n_2 = 1$ . Channel activity at a  $pH_{vac}$  of 6.0 (filled circles) was approximately 2- to 4-fold higher at all  $pH_{cyt}$  values tested, except at the extreme low ones. The  $pH_{cyt}$  activation of the channels, at  $pH_{vac}$  of 6.0, analyzed with Eq. 2 (Fig. 2b, solid line), resulted in a  $pK_{a1}$  of 6.40, and a Hill coefficient of  $n_1 = 1.2$ .  $NP_o$  was nearly completely abolished at  $pH_{cyt}$  5.0, with the inhibition kinetics resulting in a  $pK_{a2}$  of 5.44 and  $n_2 = 3$ .

The  $pK_{a1}$  values at  $pH_{vac}$  6.0 and 5.3 vary little, but the reduced Hill coefficient at  $pH_{vac} = 6.0$  suggests a very reduced degree of cooperativity among interacting ligand-binding sites during activation at this pH. The differences both in absolute activity values (Fig. 2a) and Hill coefficients at  $pH_{vac}$ 's of 5.3 and 6.0 (Fig. 2b) suggest that protonation and deprotonation of the vacuolar side of the membrane also contributes to channel regulation.

As apparent from the results shown in Fig. 1, lowering the  $pH_{cyt}$  induced an increase in the single-channel current amplitude. The single-channel current-voltage relationship showed pH dependence, but reversal potentials for the anion current were insensitive to  $pH_{cyt}$  over the range 5.0–7.2 (Fig. 3a). More detailed analysis at a pipette potential ( $V_p$ ) of +40 mV (Fig. 3b), showed that single-channel conductance increased with the decreasing  $pH_{cyt}$  in the range from 7.7 ( $G = 43.0 \pm 2.0$ ,  $N = 3$ ) to 5.0 ( $G = 62.7 \pm 0.7$ ,  $N = 12$ ). At a  $V_p$  of -40 mV, a similar increase was obtained from  $pH_{cyt}$  7.7 ( $G = 34.3 \pm 0.6$ ,  $N = 3$ ) to 5.0 ( $G = 58.9 \pm 1.1$ ,  $N = 3$ ). In both cases (Figs. 3b and c), the conductance seemed to be independent of the  $pH_{vac}$ .

**Fig. 2.** The effect of the cytosolic pH ( $pH_{cyt}$ ) on the anion channel activity. Single-channel activity was recorded from inside-out patches bathed in solutions of similar chemical composition, with different  $pH_{cyt}$  (see Table 2), and at a  $pH_{vac}$  of 5.3 (open circles) or  $pH_{vac}$  of 6.0 (filled circles). Error bars represent SEM, each data point representing an average of 3–5 independent experiments, each in a separate patch at  $V_p = +40$  mV. (a) Channel activity ( $NP_o$ ) values plotted against  $pH_{cyt}$ . (b)  $[H^+]_{cyt}$ -dependent activation and inhibition kinetics of the anion channel. Single-channel activity values were normalized ( $(NP_o)_{rel}$ ) by setting the mean channel activity values measured at  $pH_{cyt}$  6.0 to 1 and were plotted against the  $[H^+]_{cyt}$ . The solid lines represent the best fits to Eq. 2 (see the text for the resulting parameters of the fit).

#### LOW pH INCREASES $Ca^{2+}$ -SENSITIVITY OF THE ANION CHANNEL

Anion channels of the tonoplast membrane are activated by an increasing  $[Ca^{2+}]_{cyt}$ , in a concentration-dependent manner. By using solutions adjusted to  $pH_{cyt}$  7.4, the calcium activation could be characterized with a half-maximal ( $EC_{50}$ ) value for activation in the range of 100–200  $\mu M$   $Ca^{2+}$ . With  $[Ca^{2+}]_{cyt}$  levels close to the physiological range, the detected  $P_o$  of the channels was low (Berecki et al., 1999). We determined whether pH changes might have an effect on the  $Ca^{2+}$ -sensitivity of the channels. For this, we compared previously reported data of dose dependence of  $Ca^{2+}$  activation at  $pH_{cyt}$  7.4 (Berecki et al., 1999) with new data, obtained at  $pH_{vac}$  5.3/ $pH_{cyt}$  6.0 and  $pH_{vac}$  6.0/ $pH_{cyt}$  7.2, respectively (Fig. 4). Data points for  $Ca^{2+}$  activation at  $pH_{cyt}$  7.2 and 7.4 (see composition of the solutions in Table 1), fitted with Eq. 3 (solid line), revealed a Hill coefficient of  $n = 1$  and an apparent  $K_a$  ( $EC_{50}$ ) of 130  $\mu M$   $Ca^{2+}$ . Experiments performed by using solutions of  $pH_{cyt}$  6.0 and different cytosolic  $Ca^{2+}$  levels as shown in Table 1, resulted in a concentration-dependent increase of  $NP_o$ , reaching saturation already with about 10  $\mu M$   $[Ca^{2+}]_{cyt}$ . The dose-response of  $Ca^{2+}$  activation could be described with an apparent  $K_a$  ( $EC_{50}$ ) in the range of 4–6  $\mu M$   $Ca^{2+}$ , and a Hill coefficient of  $n = 2$ , suggesting an enhanced positive cooperativity, with the binding of 2  $Ca^{2+}$  ions to the anion channel protein at this more acidic pH as compared to  $pH_{cyt}$  of 7.2 and 7.4. The single-channel conductance did not change with changing  $Ca^{2+}$  concentrations.

#### VOLTAGE-DEPENDENCE OF THE ANION CHANNEL UNDER THE INFLUENCE OF $pH_{cyt}$

The effects of different membrane potentials on the opening behavior of the anion channels were examined

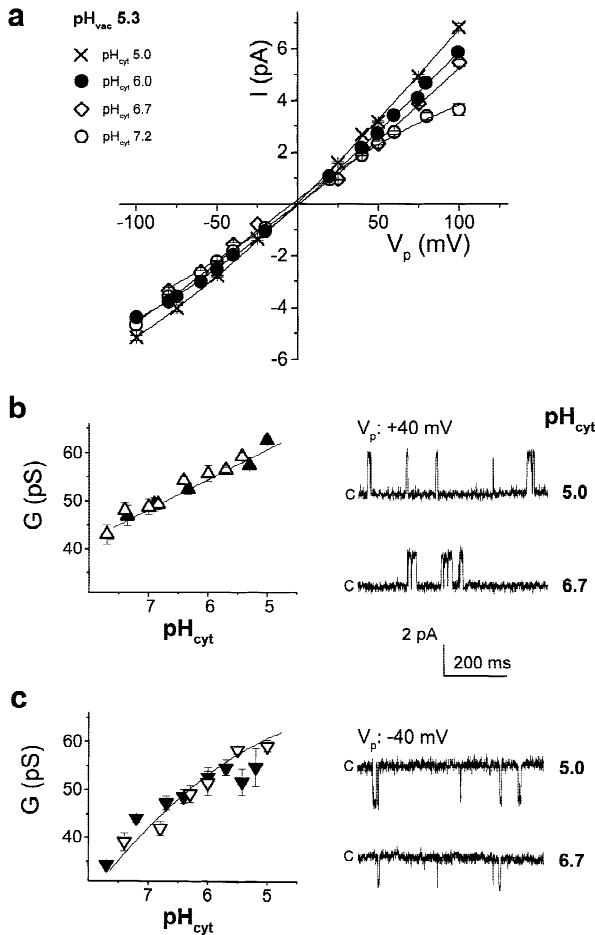


**Fig. 3.** The effect of  $\text{pH}_{\text{cyt}}$  on the anion channel conductance. (a) Single-channel openings were elicited upon applying step-pulses to the indicated pipette potential ( $V_p$ ) values from a holding  $V_p$  of 0 mV. Each point represents at least 5 determinations, each in a separate patch at  $\text{pH}_{\text{vac}} 5.3$ . The single-channel current-voltage relationships were determined for  $\text{pH}_{\text{cyt}} 5.0$  (cross),  $\text{pH}_{\text{cyt}} 6.0$  (filled circle),  $\text{pH}_{\text{cyt}} 6.7$  (diamond) and  $\text{pH}_{\text{cyt}} 7.2$  (open circle). (b) Anion channel conductance ( $G$ ) depends on  $\text{pH}_{\text{cyt}}$  (filled symbols:  $\text{pH}_{\text{vac}} 5.3$ , open symbols:  $\text{pH}_{\text{vac}} 6.0$ ). On the right: examples of single-channel recordings from an inside-out patch at  $\text{pH}_{\text{cyt}} 5.0$  and  $6.7$ , respectively. The composition of the experimental solutions is listed in Table 2,  $V_p = +40$  mV, upward deflections represent channel openings. Each point represents the mean of at least three independent experiments. (c) The same experiments as shown in b, but  $V_p = -40$  mV, downward deflections represent channel openings.

(Fig. 5). We applied both short (2 sec) and long (25 sec) voltage steps (from a holding potential of 0 mV to the indicated  $V_p$ ) to the membrane patches. At low  $\text{pH}_{\text{cyt}}$  (6.0), channel activity showed voltage-dependence with higher activity for more positive  $V_p$ , as shown in the left-hand-side current traces in Fig. 5a and  $\text{NP}_o$  values in Fig. 5b. The  $\text{NP}_o$  did not change in the  $V_p$  range from  $-100$  to  $+20$  mV. However, at more positive  $V_p$  values, up to  $+140$  mV, activity gradually increased, from a relatively low- to a high-activity state. Saturation of the ac-

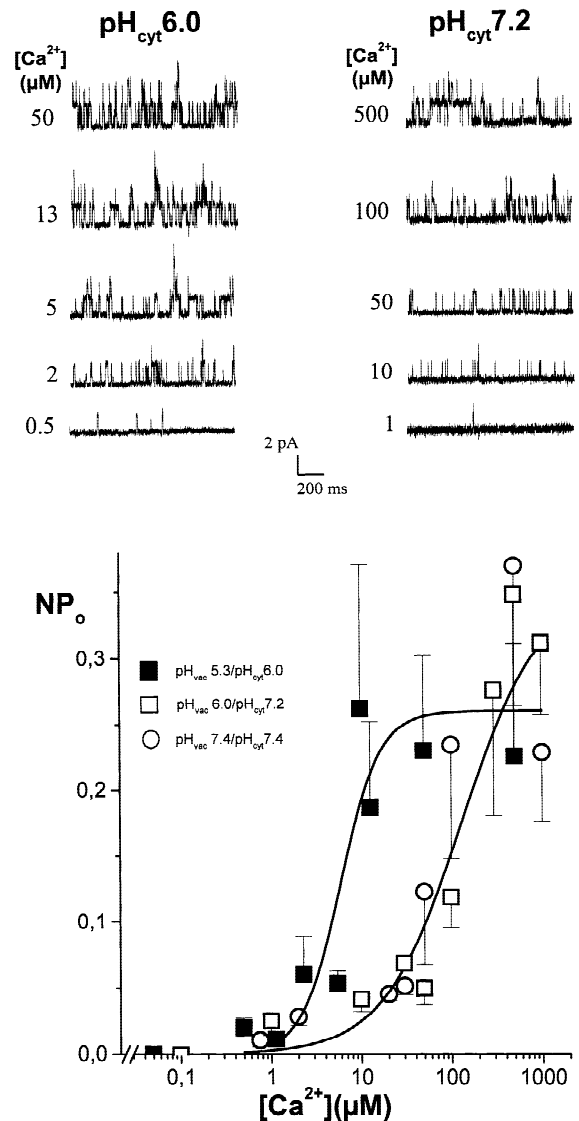


**Fig. 4.** Calcium-sensitivity of  $\text{NP}_o$  at  $\text{pH}_{\text{cyt}}$  of 6.0 (filled squares), 7.2 (open squares) and 7.4 (open circles). Current traces shown all represent independent experiments during which perfusion was omitted; the  $V_p$  was  $+40$  mV. Inside-out patches were bathed in solutions of compositions shown in Table 1. Error bars represent SEM; each point represents 3–5 determinations, each in a separate patch. With  $\text{pH}_{\text{cyt}}$  of 6.0 and 7.2, the conductance of the channel was  $55 \pm 0.7$  pS ( $N = 17$ ) and  $51.9 \pm 0.5$  pS ( $N = 18$ ), respectively. Data points were best fitted (solid lines) using Eq. 3, with  $n = 2$  and  $K_a$  of  $5 \mu\text{M}$  ( $\text{pH}_{\text{cyt}} 6.0$ ) and  $n = 1$  and  $K_a$  of  $130 \mu\text{M}$  ( $\text{pH}_{\text{cyt}} 7.2$  and  $\text{pH}_{\text{cyt}} 7.4$ ). Results obtained at  $\text{pH}_{\text{cyt}} 7.4$  (Berecki et al., 1999) were updated with additional points (at 30 and  $50 \mu\text{M}$   $[\text{Ca}^{2+}]_{\text{cyt}}$ ), while data recorded in the presence of very high  $[\text{Ca}^{2+}]_{\text{cyt}}$  (5 mM, Berecki et al., 1999) were not included.

tivity could not be reached in these experiments, as at  $V_p$  values of  $+120$  and  $+140$  mV new channels could still be recruited (*data not shown*). At a  $V_p$  of  $+100$  mV, channel activity was approximately 15 times higher than at negative pipette potentials.

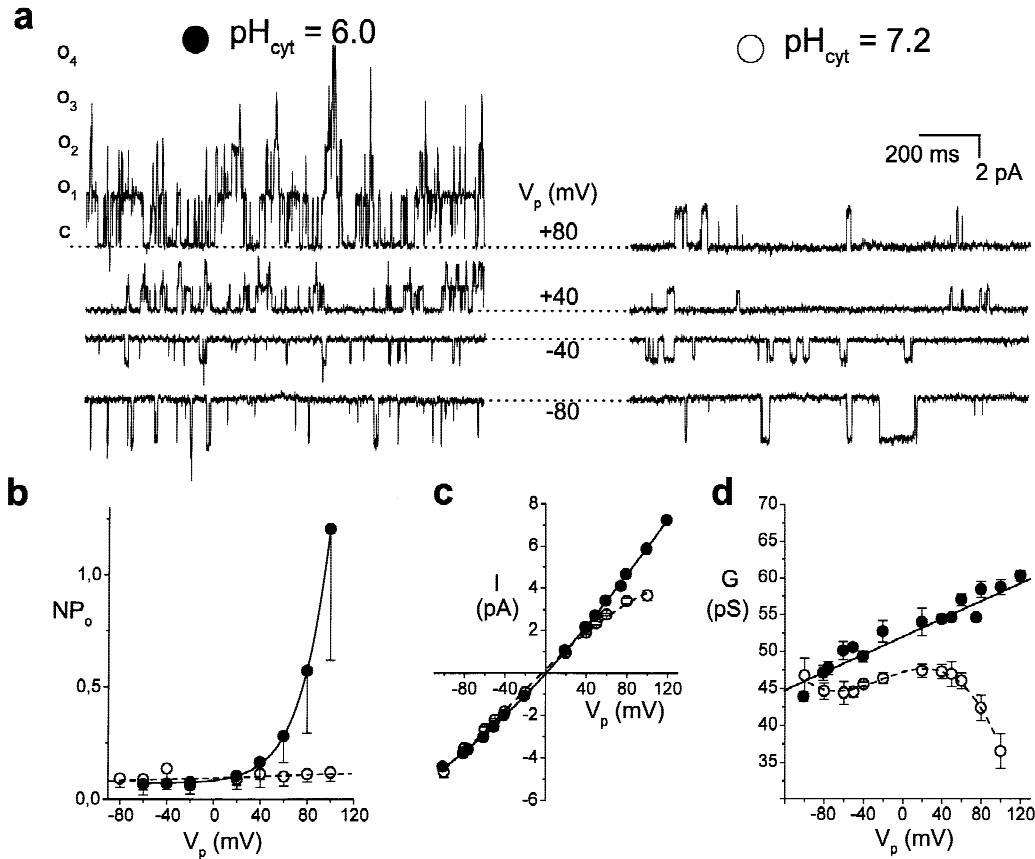


**Fig. 5.** Voltage-dependence of the  $NP_o$ , with  $pH_{vac} = 5.3$ . The composition of the experimental solutions is shown in Table 2. To increase  $P_o$  at  $pH_{cyt} 7.2$ ,  $[Ca^{2+}]_{cyt}$  was adjusted to  $500 \mu M$ ; solid circles:  $pH_{cyt} 6.0$ , open circles:  $pH_{cyt} 7.2$  (a) Current recordings from inside-out patches, with the  $V_p$  stepped to the indicated  $V_p$ 's from a holding-potential value of 0 mV. Dotted lines indicate current levels when the channels are closed; superimposed individual channels are numbered continuously ( $O_1, \dots, O_4$ , at +80 mV). (b)  $NP_o$  depends on  $V_p$ . Mean values  $\pm$  SEM, obtained at different pipette potentials ( $V_p$ ) are shown; the  $pH_{cyt}$  was either 6.0 (filled circles,  $N = 5$ ) or 7.2 (open circles,  $N = 3$ ). Pipette potentials in the range from  $-80$  to  $+100$  mV were applied. To guide the eye, data points were fitted with a sigmoidal (Boltzmann-type eq.) and a linear line, respectively. (c) Single-channel current-voltage relationships (for details, see Fig. 3a). (d) Voltage-dependence of the single-channel conductance at  $pH_{cyt} 6.0$  (solid circles,  $N = 11$ ) or  $pH_{cyt} 7.2$  (open circles,  $N = 7$ ), respectively.  $V_p$ 's in the range from  $-100$  to  $+120$  mV were applied; Data points were fitted with a linear function (solid line) and with a 3rd-order polynomial function, respectively (dotted line).

At  $pH_{cyt} 7.2$ , activity and the opening behavior seemed to be independent of the applied  $V_p$  (see right-hand-side current traces shown in Fig. 5a and  $NP_o$  values shown in Fig. 5b).

The single-channel current-voltage relationships (Fig. 3a), replotted for  $pH_{cyt}$  of 6.0 and 7.2, respectively, suggested voltage-dependence (Fig. 5c). This was evident from the conductance-voltage relationships, with the single-channel conductance ( $G$ ) being voltage-dependent at both  $pH_{cyt} 6.0$  and 7.2 (Fig. 5c). At a  $pH_{cyt}$  of 6.0,  $G$  values showed a monotonic increase as  $V_p$  became more positive. At  $pH_{cyt}$  of 7.2, the applied  $V_p$  in the  $V_p$  range from  $-100$  to  $+60$  mV did not significantly influence  $G$  values. At more positive  $V_p$ 's single-channel conductance decreased in a voltage-dependent manner.

#### MEAN OPEN TIMES

From our single-channel recordings (see Fig. 1) it was difficult to assess how  $N$  and  $P_o$  are separately affected

by the changing  $pH_{cyt}$ . The elemental variable,  $P_o$ , is partly determined by the channel open time. As the tonoplast anion channel activity shows  $Ca^{2+}$ -,  $pH$ - and voltage-dependence, we studied the effect of these parameters on the single-channel open times. Fig. 6 shows that in the  $pH_{cyt}$  range between 4.1 and 8.7, the anion channels exhibited gating behavior that mostly required two exponentials to fit the channel dwell-time distributions (see Methods). At  $pH_{cyt} 5.0$  the time constant of the shorter open state,  $\tau_1$ , was about 1.8 msec, while the time constant of the longer open state,  $\tau_2$ , had a value of about 18 msec. Towards higher  $pH_{cyt}$  values both time constants decreased. At  $pH_{cyt} 8.7$ , the dwell-time distribution could be best fitted by a single exponential function, indicating that the fast component was inactivated (Fig. 6c).

At  $pH_{cyt} 6.0$  and low  $[Ca^{2+}]_{cyt}$ , anion channels display voltage-dependent gating, as  $\tau_2$  (the longer open-time component) decreased towards more negative  $V_p$

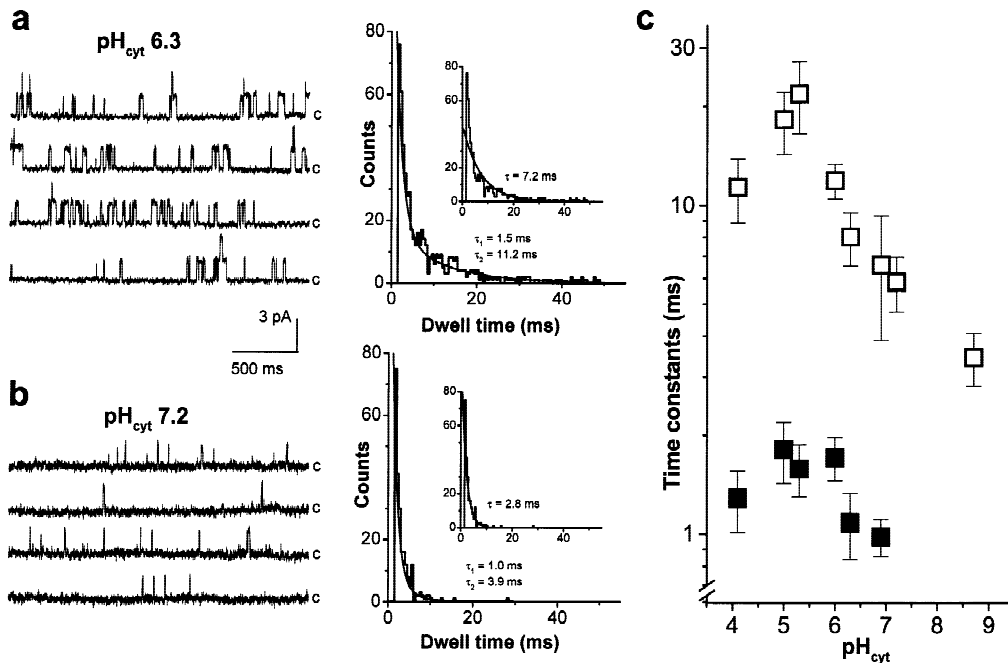


**Fig. 6.** Low  $\text{pH}_{\text{cyt}}$  increases the open time of the anion channel. Representative single-channel current traces from two inside-out patches, bathed in solutions (see Table 2. for the composition) of  $\text{pH}_{\text{cyt}}$  6.3 (a) and  $\text{pH}_{\text{cyt}}$  7.2 (b), respectively, are shown. The closed state of the channel (C) is indicated; the scale is similar for all traces;  $V_p$ : +40 mV. Open dwell-time histograms for a and b were fitted in pCLAMP 6 (solid lines), with double- or single- (see insets) exponential functions. The resulting time constants are shown. (c) The means ( $\pm$  SEM) for the time constants  $\tau_1$  (filled square) and  $\tau_2$  (open square), obtained after fitting the dwell-time histograms, were plotted against the  $\text{pH}_{\text{cyt}}$ . The mean  $\tau_1$  value, obtained at  $\text{pH}_{\text{cyt}}$  7.2, was not included, because after fitting either with a single- or double-exponential function and assessing the fit (see Methods), we could not choose a better model (in both cases the Schwartz-criterion showed almost identical values). Data point at  $\text{pH}_{\text{cyt}}$  7.2 represents the averaged  $\tau_2$  value. Each point represents the mean of three to five experiments.

(Fig. 7a). The faster time constant,  $\tau_1$ , showed less voltage-dependence. These results suggest that the increase in the mean open times towards positive  $V_p$ 's at least partly accounts for the voltage-dependent increase of the anion channel activity at low  $\text{pH}_{\text{cyt}}$  (see Fig. 5b). When higher cytoplasmic calcium concentrations were used, at  $\text{pH}_{\text{cyt}}$  6.0, open-time constants still showed an increase towards positive  $V_p$  values, although the voltage dependence was weaker compared to the situation with low  $[\text{Ca}^{2+}]_{\text{cyt}}$  (Fig. 7a). This suggests a regulatory role in gating of the channel not only for pH but for  $\text{Ca}^{2+}$  as well. Our analysis of the time constants at  $\text{pH}_{\text{cyt}}$  of 7.2, in the presence of a relatively high cytoplasmic calcium concentration (500  $\mu\text{M}$ ), revealed that the open-time durations displayed two exponents with no significant voltage dependency (Fig. 7b). Changing the  $\text{pH}_{\text{vac}}$  did not affect this absence of voltage-dependence, although  $\tau_2$  values were slightly increased at more acidic  $\text{pH}_{\text{vac}}$  (5.3 versus 6.0).  $\text{Ca}^{2+}$ -sensitivity of voltage-dependence of the open times at a  $\text{pH}_{\text{cyt}}$  of 7.2 could not be analyzed, as we were unable to produce adequate data by using low  $[\text{Ca}^{2+}]_{\text{cyt}}$  at this  $\text{pH}_{\text{cyt}}$  value (see Fig. 2). However, the effect of  $[\text{Ca}^{2+}]_{\text{cyt}}$  on the time-constant values at  $\text{pH}_{\text{cyt}}$  of 7.2 can be estimated by comparing the  $\tau_1$  and  $\tau_2$  values found at  $\text{pH}_{\text{cyt}}$  7.2, in the presence of 50  $\mu\text{M}$   $\text{Ca}^{2+}$  (Fig.

6), with the  $\tau_1$  and  $\tau_2$  values determined in the presence of 500  $\mu\text{M}$   $\text{Ca}^{2+}$ , at +40 mV (Fig. 7). In the latter case  $\tau_1$  and  $\tau_2$  were approximately 3- and 4-fold larger, respectively.

## Discussion

### $\text{H}^+$ -DEPENDENCY OF THE ANION CHANNEL

Acidification of defined endomembrane compartments is essential for plant cellular functions and provides driving force for the secondary transport of a variety of ions and metabolites (Sze, 1985). On the other hand, acidification of the cytosol is generally associated with various stress situations, leading to metabolic disruptions, increasing cellular levels of  $\text{Ca}^{2+}$  and the pH-dependent activation of enzyme cascades (Kinnersley & Turano, 2000).

The present study demonstrates that anion channels of the tonoplast of *C. corallina* are sensitive to both cytosolic and vacuolar pH. The pH-dependence was reversible, as demonstrated by subsequent inhibitions and activations of the channels in the same patch (Fig. 1). Acidification of the cytosolic side of the membrane first



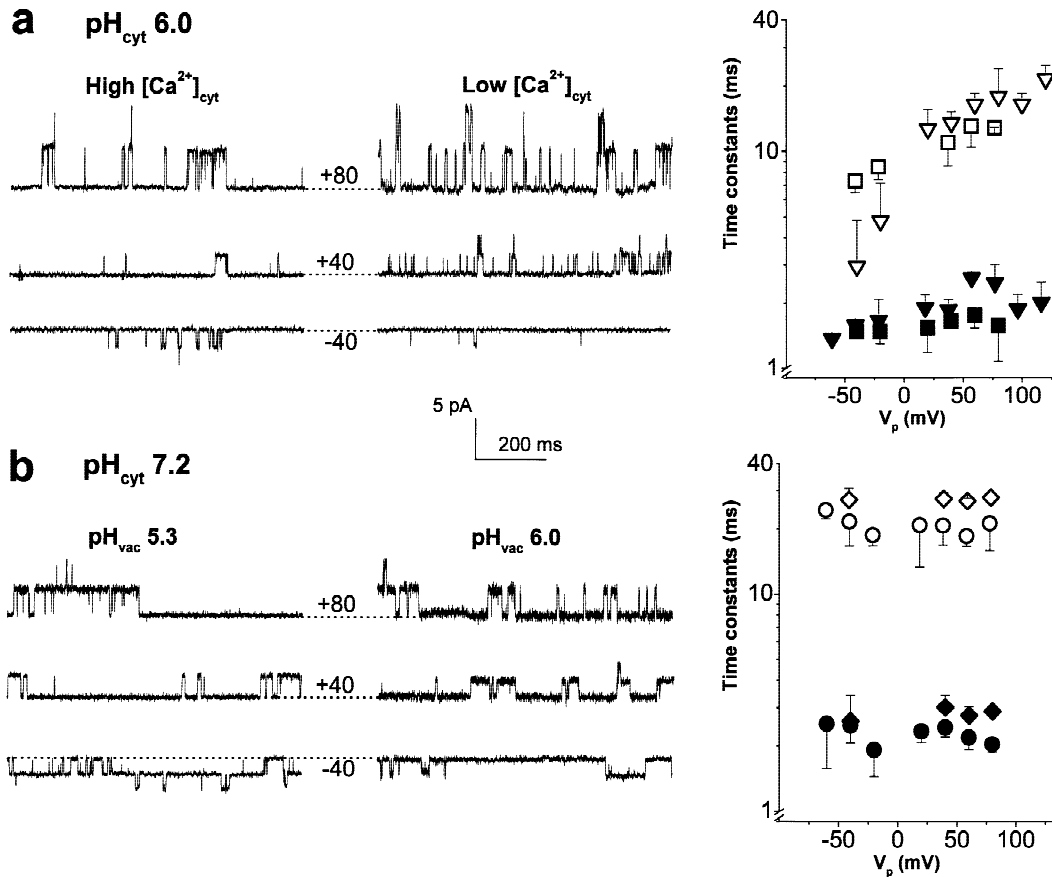


**Fig. 7.** Voltage-dependence of the mean open time. Representative single-channel current traces are displayed on the left. The means ( $\pm$  SEM) for  $\tau_1$  (filled symbols) and  $\tau_2$  (open symbols), resulting after fitting of the dwell-time histograms, are plotted against the applied pipette potentials ( $V_p$ ). The closed state of the channel is marked by dotted lines. (a) With low  $[Ca^{2+}]_{cyt}$  (in the range between 1 and 50  $\mu$ M, see Table 1), time constants (triangles) showed a marked voltage-dependence. With high  $[Ca^{2+}]_{cyt}$  (500  $\mu$ M and 1 mM), the voltage-dependence is weaker (squares). Each point represents the mean of three to seven experiments. (b) At  $pH_{cyt}$  7.2 (diamond:  $pH_{vac}$  5.3; circle:  $pH_{vac}$  6.0) the time constants were not voltage-dependent. Each point represents the mean of three to four experiments.

induced an activity increase with an apparent recruitment of new channels. (Figs. 1 and 2). The conductance of the single channels was independent of the  $pH_{vac}$  but higher when the  $pH_{cyt}$  was low (Fig. 3). The activation and inhibition of the channels by increasing proton concentrations at the cytosolic side could be described by sigmoidal kinetics, considering that two opposing processes are involved. In classical terms, with an  $n$  (Hill-coefficient)  $> 1$ , the binding of the first  $H^+$  induces a conformational change, which increases the affinity for the binding (or the release) of the second  $H^+$  (allosteric effect). The highest channel activity was found at  $pH_{cyt}$  6.0. Going from high to low  $pH_{cyt}$ , activation was followed by the inhibition of the channel at very acidic  $pH_{cyt}$  below 6.0 (Fig. 2). During activation, the apparent dissociation constants ( $K_{a1}$ ) at different fixed  $pH_{vac}$  (5.3 and 6.0, Fig. 2) showed a similar value of 6.4. However,  $n_1$  was either about 1 or 4. When the  $pH_{vac}$  was higher, the cooperativity was weaker. The higher  $n$  value sug-

gests an increased avidity and the presence of a number of identical  $H^+$  binding sites on the channel protein. In addition, our data show that the channel is sensitive to both cytosolic and vacuolar pH.

The effect of  $Ca^{2+}$  on the tonoplast anion channels has been reported previously (Berecki et al., 1999). Low  $pH_{cyt}$  caused an improved binding of  $Ca^{2+}$  ions to the channel protein without affecting channel conductance (Fig. 4). Results of these experiments, together with previous findings (Berecki et al. 1999) show that the apparent dissociation constant of  $Ca^{2+}$  binding ( $K_a$ ) decreases when the  $pH_{cyt}$  is lowered, resulting in an increased  $Ca^{2+}$ -sensitivity of the channels.

At low  $pH_{cyt}$ , the membrane potential was a potent regulator of the anion channel activity (Fig. 5). When positive pipette potentials were applied, corresponding to hyperpolarization of the tonoplast membrane, channel activity increased dramatically. However, at  $pH_{cyt}$  7.2 voltage-dependence of channel activity was absent. The

voltage-dependence of the single-channel conductance was also  $\text{pH}_{\text{cyt}}$ -dependent. At  $\text{pH}_{\text{cyt}}$  6.0, smaller conductances were recorded at negative pipette potentials, and the conductance showed a linear increase towards positive  $V_p$ 's, while, at  $\text{pH}_{\text{cyt}}$  7.2, the voltage-dependence of the conductance was evident (decreasing) only at extreme positive  $V_p$ 's (Fig. 5d), suggesting a fast block of the channels by an electric screening of surface charges (Hille, 1992). One of the consequences of such a "titration" effect would be a shift of the observed reversal potential (Hille, 1992). However, since the reversal potential is insensitive to  $\text{pH}_{\text{cyt}}$  (Fig. 3a), we conclude that this mechanism is not responsible for the observed reduction of the channel conductance.

In our experiments,  $NP_o$  could be increased in several ways (pH decrease, positive  $V_p$ 's at low  $\text{pH}_{\text{cyt}}$  or increase of the  $[\text{Ca}^{2+}]_{\text{cyt}}$ ). According to almost any model of gating, the total current (reflected in  $NP_o$ ) should become larger when inactivation is removed (Hille, 1992). During the experiment shown in Fig. 1, with unchanged  $[\text{Ca}^{2+}]_{\text{cyt}}$  and  $V_p$ , the pH-dependence of the  $NP_o$  is likely to also involve new channel recruitment. Simply altering the open-times of individual channels by  $\text{pH}_{\text{cyt}}$  decrease (from 7.4 to 6.0) cannot account for the magnitude of the  $NP_o$  change observed (Fig. 6).

Results shown in Fig. 7a demonstrate a  $V_p$ -dependent modulation of the anion channel open time. However, also here, in the  $V_p$  range between +20 and +100 mV, the increase of the mean open times seems to be too trifling to explain the dramatic increase of  $NP_o$  at low  $\text{pH}_{\text{cyt}}$  (Fig. 5a, b). The magnitude of the anion flux detected at extreme positive voltages suggests that the increase of the mean open time (Fig. 7a) could not be alone responsible for the approx. 15-fold increase of  $NP_o$ . Therefore, more likely, the activation involves mobilization of channels from an inactivated ("sleepy") (Hille, 1992) state to an activated state. As a result, the number of channels available for activation increases. Thus,  $[\text{H}^+]$  controls the number of channels that can enter the pool available for voltage-dependent activation. Similar hypotheses of pH-induced channel recruitment appear in the literature, e.g., for the inward-rectifier  $\text{K}^+$  channel of *Vicia* guard cells (Grabov & Blatt, 1997) or for the *Arabidopsis* outwardly-rectifying  $\text{K}^+$  channel SKOR (Lacombe et al., 2000).

Besides voltage and pH,  $[\text{Ca}^{2+}]_{\text{cyt}}$  seems to be an important factor involved in the regulation of  $NP_o$ . However, apart from the conclusion that  $\text{Ca}^{2+}$  causes an increase of the open time (Figs. 6 and 7), we are not able to provide a more detailed characterization of the  $\text{Ca}^{2+}$ -induced modifications of the channel gating.

#### PHYSIOLOGICAL ROLE

At a physiological  $\text{pH}_{\text{cyt}}$  (around 7.4), anion channels are hardly available for activation. But lowering of the cy-

tosolic pH increases all activity parameters (including  $\text{Ca}^{2+}$ -sensitivity) and induces a voltage-dependence of the tonoplast anion channels. The physiological significance of the pH-regulated anion channels of the tonoplast is still to be established. A general model of the plasma membrane transporters in plants shows that the osmotic balance in these cells is achieved with nonlinear oscillations of a dynamic system made up of a number of membrane voltage and  $[\text{H}^+]$  sensitive elements (Gradmann, Blatt & Thiel, 1993). It can be expected that similar electrocoupling of the tonoplast ion transporters exists in the large internodal cells, driving osmotic events. An acidic  $\text{pH}_{\text{cyt}}$  could trigger a series of events which ultimately would lead to modulation of ion channels. In addition,  $\text{Ca}^{2+}$ -release following cytosolic acidification might be a key signal for the turgor regulation in *Chara*. The importance of voltage-dependence of the anion channels seems to be less significant, considering that the magnitude of tonoplast membrane potential changes that occur during an action potential (about  $\pm 20$  mV) are small, as compared with the plasma membrane action potential (Kikuyama, 1986). Tester, Beilby & Shimmen (1987) showed that reducing pH by one unit (to  $\text{pH}_{\text{cyt}}$  6.6) had little effect on tonoplast membrane potential in permeabilized cells of *Chara corallina*, perhaps depolarizing the tonoplast by only about 0.5 mV. Beilby (1990) showed that depletion or buildup of ions during slow ramp command determines the  $I/V$  characteristics of the *Chara* plasma membrane and alters the ionic concentrations at the membrane/media interfaces in the immediate membrane vicinity. In analogy, the tonoplast proton pump activity could also cause significant differences in the pH along and in the vicinity of the *Chara* tonoplast.

The current knowledge about the electrophysiological properties and modulation of both channels and vacuolar pumps in the *Chara* tonoplast opens now the way for mathematical modelling of this membrane. Such a model would provide a deeper understanding of the tonoplast ion fluxes in response to changing environmental conditions.

The work was supported by a grant from the Dutch Platform "Alternatives for Animal Experimentation" (ZON 9802.036.0).

#### References

- Allen, G.J., Sanders, D. 1996. Control of ionic currents in guard cell vacuoles by cytosolic and luminal calcium. *Plant J.* **10**:1055–1069
- Allen, G.J., Amtmann, A., Sanders, D. 1998. Calcium-dependent and calcium-independent  $\text{K}^+$  mobilization channels in *Vicia faba* guard cell vacuoles. *J. Exp. Bot.* **49**:305–318
- Beilby, M.J. 1990. Current-voltage curves for plant membrane studies: a critical analysis of the method. *J. Exp. Bot.* **41**:165–182
- Berecki, G., Varga, Z., Van Iren, F., Van Duijn, B. 1999. Anion channels in *Chara corallina* tonoplast membrane: calcium dependence and rectification. *J. Membrane Biol.* **172**:159–168
- Berecki, G., Eijken, M., Van Iren, F., Van Duijn, B. 2001. Membrane

- orientation of droplets prepared from *Chara* internodal cells. *Protoplasma*. **218**:76–82
- Bertl, A., Blumwald, E., Coronaro, R., Eisenberg, R., Findlay, G., Gradmann, D., Hille, B., Köhler, K., Kolb, H.A., MacRobbie, E., Meissner, G., Miller, C., Neher, E., Palade, P., Pantoja, O., Sanders, D., Schroeder, J., Slayman, C., Spanswick, R., Walker, A., Williams, A. 1992. Electrical measurements on endomembranes. *Science* **258**:873–874
- Blatt, M.R. 1987. Electrical characteristics of stomatal guard cells: The contribution of ATP-dependent, electrogenic transport revealed by current-voltage and difference-current-voltage analysis. *J. Membrane Biol.* **98**:257–274
- Colquhoun, D., Sigworth, F.J. 1983. Fitting and statistical analysis of single-channel records. In: Single-Channel Recording. B. Sakmann and E. Neher, editors. pp. 191–263. Plenum Press, New York
- Felle, H. 1988. Cytoplasmic free calcium in *Riccia fluitans* L. and *Zea Mays* L.: Interaction of  $\text{Ca}^{2+}$  and pH? *Planta* **176**:248–255
- Felle, H. 1989. pH as a second messenger in plants. In: Second messengers in plant growth and development. W.F. Boss and D.J. Morre, editors. pp. 145–166. Alan R. Liss Inc, New York
- Gilroy, S., Bethke, P.C., Jones, R.L. 1993. Calcium homeostasis in plants. *J. Cell Sci.* **106**:453–462
- Glickman, J., Croen, K., Kelly, S., Al-Awquati, Q. 1983. Golgi membranes contain an electrogenic  $\text{H}^+$  pump in parallel to a chloride conductance. *J. Cell Biol.* **97**:1303–1308
- Grabov, A., Blatt, M.R. 1997. Parallel control of the inward-rectifier  $\text{K}^+$  channel by cytosolic  $\text{Ca}^{2+}$  and pH in *Vicia* guard cells. *Planta* **201**:84–95
- Grabov, A., Blatt, M.R. 1998. Coordination of signalling elements in guard cell ion channel control. *J. Exp. Bot.* **49**:351–360
- Gradmann, D., Blatt, M.R., Thiel G. 1993. Electrocoupling of ion transporters in plants. *J. Membrane Biol.* **136**:327–332
- Hamill, O.P., Marty, A., Neher, E., Sakmann, B., and Sigworth, F.J. 1981. Improved patch-clamp techniques for high-resolution current recording from cells and cell-free membrane patches. *Pflügers Arch.* **391**:85–100
- Hille, B. 1992. Ionic channels of excitable membranes. Sinauer Associates, Sunderland, MA
- Keunecke, M., Hansen, U.P. 2000. Different pH-dependences of  $\text{K}^+$  channel activity in bundle sheath and mesophyll cells of maize leaves. *Planta* **210**:792–800
- Kikuyama, M. 1986. Tonoplast action potential in Characeae. *Plant Cell Physiol.* **27**:1461–1468
- Kinnersley, A.M., Turano, F.J. 2000. Gamma aminobutyric acid (GABA) and plant responses to stress. *Crit. Rev. Plant Sci.* **19**:479–509
- Klieber, H.G., Gradmann, D. 1993. Enzyme kinetics of the prime  $\text{K}^+$  channel in the tonoplast of *Chara*: selectivity and inhibition. *J. Membrane Biol.* **132**:253–265
- Koshland, D.E., Némethy, G., Filmer, D. 1966. Comparison of experimental binding data and theoretical models in proteins containing subunits. *Biochemistry* **5**:365–385
- Kurkdjian, A., Guern, J. 1989. Intracellular pH: measurement and importance in cell activity. *Annu. Rev. Plant Physiol. Plant Mol. Biology* **40**:271–303
- Laver, D.R., Walker, N.A. 1991. Activation by  $\text{Ca}^{2+}$  and block by divalent ion of the  $\text{K}^+$  channel from *Chara australis*. *J. Membrane Biol.* **120**:131–139
- Lacombe, B., Pilot, G., Gaymard, F., Sentenac, H., Thibaud, J.B. 2000. pH control of the plant outwardly-rectifying potassium channel SKOR. *FEBS Lett.* **466**:351–354
- Lüthring, H. 1999. pH-sensitive gating kinetics of the maxi-K channel in the tonoplast of *Chara australis*. *J. Membrane Biol.* **168**:47–61
- McAinsh, M.R., Brownlee, C., Hetherington, A.M. 1990. Absciscic acid-induced elevation of guard cell cytosolic  $\text{Ca}^{2+}$  precedes stomatal closure. *Nature* **343**:186–188
- Moriyasu, Y., Shimmen, T., Tazawa, M. 1984. Vacuolar pH regulation in *Chara australis*. *Cell Struct. Funct.* **9**:225–234
- Plieth, C., Sattelmacher, B., Hansen, U.-P. 1997. Cytoplasmic  $\text{Ca}^{2+}$ - $\text{H}^+$ -exchange buffers in green algae. *Protoplasma* **198**:107–124
- Schroeder, J.I., Hagiwara, S. 1989. Cytoplasmic calcium regulates ion channels in the plasma membrane of *Vicia faba* guard cells. *Nature*. **338**:427–430
- Schultz-Lessdorf, B., Hedrich, R. 1995. Protons and calcium modulate SV-type channels in the vacuolar-lysosomal compartment-channel interaction with calmodulin inhibitors. *Planta* **197**:655–671
- Schultz-Lessdorf, B., Lohse, G., Hedrich, R. 1996. GCAC1 recognizes the pH gradient across the plasma membrane: a pH-sensitive and ATP-dependent anion channel links guard cell membrane potential to acid and energy metabolism. *Plant J.* **10**:993–1004
- Schwartz, G. 1978. Estimating the dimension of a model. *Ann. Statistics* **6**:461–464.
- Sigworth, F., Sine S. 1987. Data transformation for improved display and fitting of single channel dwell time histograms. *Biophys. J.* **52**:1047–1054
- Sze, H. 1985.  $\text{H}^+$ -translocating ATPases: advances using membrane vesicles. *Annu. Rev. Plant Physiol. Plant Mol. Biol.* **36**:175–208.
- Takeshige, K., Tazawa, M., Hager, A. 1988. Characterization of the  $\text{H}^+$ -translocating adenosine triphosphatase and pyrophosphatase of vacuolar membranes isolated by means of perfusion technique from *Chara corallina*. *Plant Physiol.* **86**:1168–1173
- Tazawa, M., Kikuyama, M., Shimmen, T. 1976. Electric characteristics and cytoplasmic streaming of characean cells lacking tonoplast. *Cell Struct. Funct.* **1**:165–176
- Tester, M., Beilby, M.J., Shimmen, T. 1987. Electrical characteristics of the tonoplast of *Chara corallina*: a study using permeabilised cells. *Plant Cell Physiol.* **28**:1555–1568
- Tyerman, S.D., Findlay, G.P. 1989. Current-voltage curves of single  $\text{Cl}^-$  channels which coexist with two types of  $\text{K}^+$  channel in the tonoplast of *Chara corallina*. *J. Exp. Bot.* **40**:105–117
- Ward, J.M., Schroeder, J.I. 1994. Calcium activated  $\text{K}^+$  channels and calcium induced calcium release by slow vacuolar ion channels in guard vacuoles implicated in the control of stomatal closure. *Plant Cell* **6**:669–683